Lithology, dynamism and volcanic successions at Melka Kunture (Upper Awash, Ethiopia)

Jean-Paul Raynal, Guy Kieffer

Edited by
Jean Chavaillon and Marcello Piperno

Studies on the Early Paleolithic site of Melka Kunture, Ethiopia

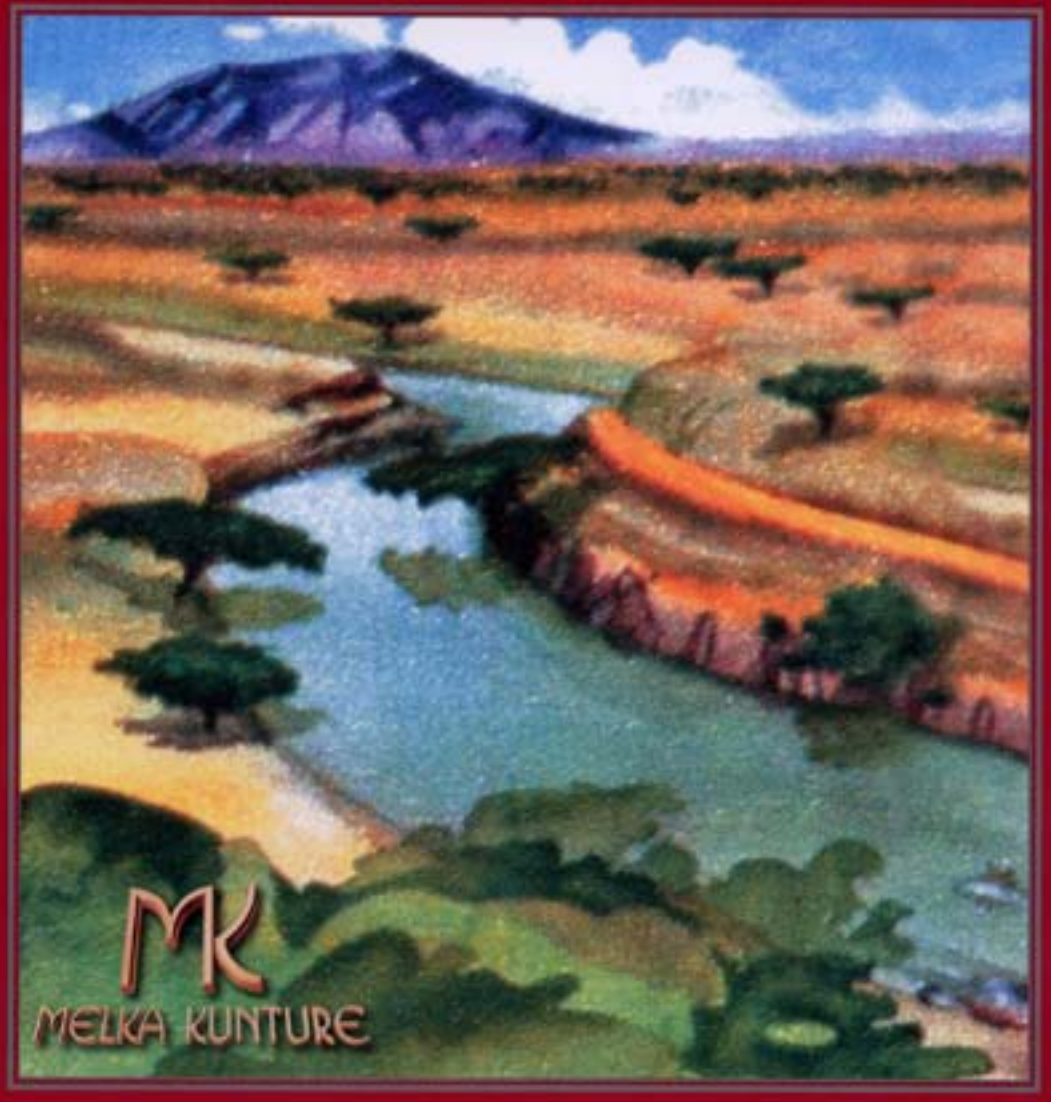

ORIGINES Studies and materials published by the Istituto Italiano di Preistoria e Protostoria

Studies on the Early Paleolithic site of Melka Kunture, Ethiopia
Edited by
Jean Chavaillon and Marcello Piperno

*

Geology, volcanology and geochemistry

Geology, volcanology and geochemistry

Lithology, dynamism and volcanic successions at Melka Kunture (Upper Awash, Ethiopia)

Jean-Paul Raynal[1], Guy Kieffer[2]

Lying some fifty kilometres south of Addis Ababa, the studied area belongs to the Ethiopian Plateau and is adjacent to the Main Ethiopian Rift, between the Ambo lineament on the north with the Wachacha and Furi volcanoes, and the Guraghe Mounts in the south (Fig. 1).

Vulcanism of the Melka Kunture area was an event with multiple eruptions, correlating with the Mio-Plio-Pleistocene evolution of the Ethiopian Rift of which ancient episodes remain in the landscape as partly basaltic residual hills. This very first volcanic event, whose outliers are very eroded, may belong to one or several eruptive phases identified elsewhere in the evolutionary context of the Ethiopian Rift.

Here we distinguish between two different and successive volcanic events: the initial vulcanism set up on the regional fault network and a different distal facies linked to further vulcanism. This distal vulcanism can be observed either as direct fallout or as reworked products that formed tuffaceous beds and which complicate the interpretation of any specific volcanic event.

The initial vulcanism expressed itself in the Melka Kunture area, which of course does not exclude the presence of prior volcanic products of distant origin, locally outcropping at the base of some geological sections. The rest of the volcanic succession is mainly formed of acidic lavas often grading into rhyolites rich in silica. Among the lithological types represented *in situ*, in flows or fragments among projections or alluvial deposits, a good proportion of ignimbrites with various facies is evident.

Our observations allow us to outline the succession and characteristics of the eruptive phases whose products affected the archaeological sites of Melka Kunture. We indicate the main episodes, which are those that left massive deposits and were most involved in the history and conservation of the sites. However, many sections show that several other phases, of various importance, ejected their products into this area and would complicate this outline if we took every one of them into account.

1. Université de Bordeaux 1, Institut de Préhistoire et de Géologie du Quaternaire, UMR 5199 CNRS, Avenue des Facultés, F- 33405 Talence et GDR 1122 CNRS, France. jpraynal@wanadoo.fr. 2. UMR 6042 CNRS, Université Blaise Pascal, Maison de la Recherche, 4 rue Ledru, 63057 Clermont-Ferrand Cedex 1, Centre de Recherches Volcanologiques et GDR 1122 CNRS.

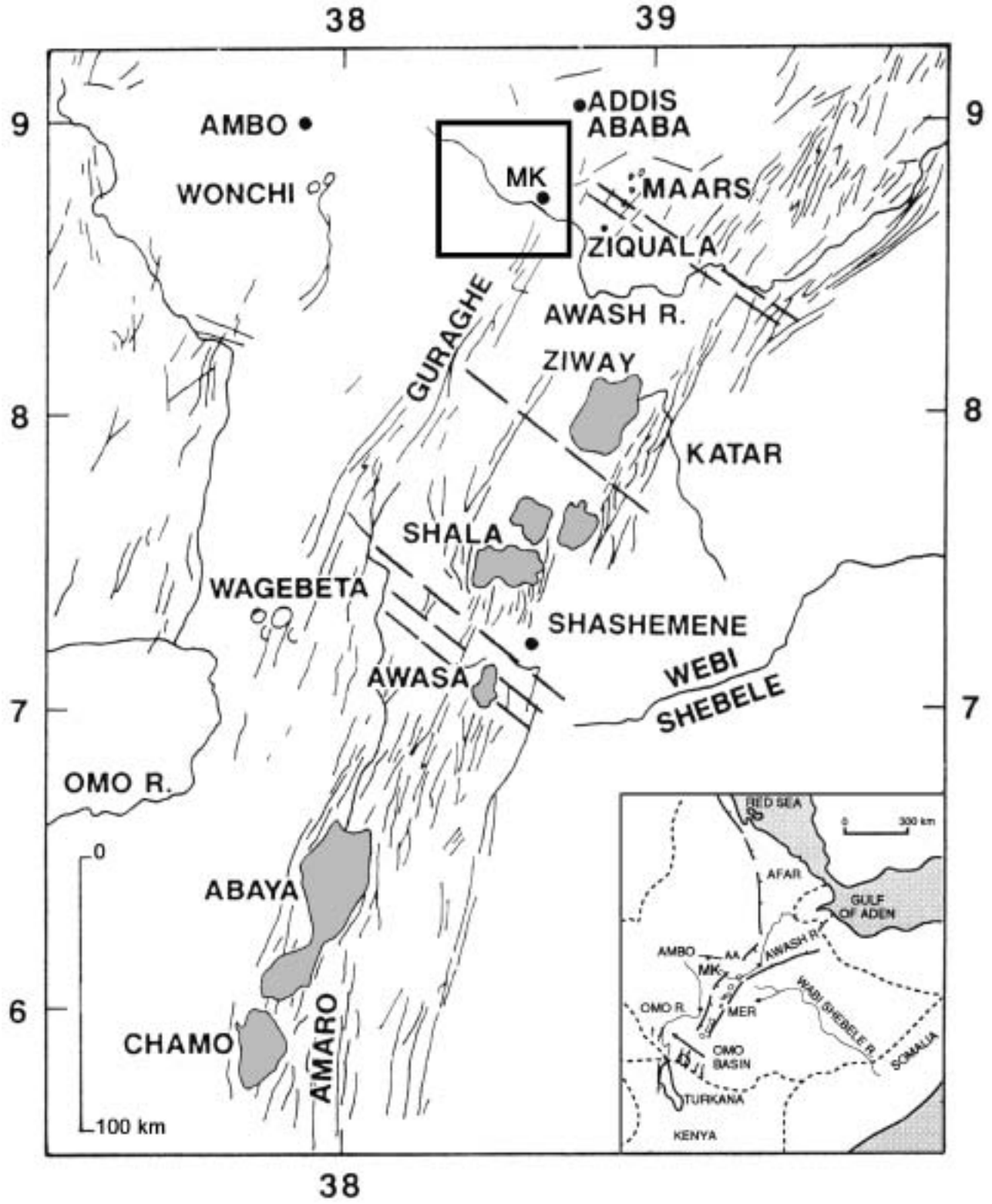

Fig. 1. Location map for the Melka Kunture area (after Woldegabriel *et al.* 1990).

Fig. 2. Lava lake remnants in Awash gorges at Meka Kunture. *Cliché J.-P. Raynal*

The initial volcanic events

In the Melka Kunture area, these begin with an activity aligned on a system of faults visible in the southern part of the Awash River basin. Here, we see eruptive cycles of differentiated fluidal aphyric lavas, of benmoreitic aspect, which are also visible in the Awash gorges as far as to the Simbiro gully. At the Melka Kunture ford the lava lake appears to have been several tens of metres thick, and several hundred metres wide, which could have occupied a crater structure of phreatomagmatic origin (Fig. 2).

In the Simbiro gully, we find remains of another laval exit point, established on a fault segment parallel to that of Melka Kunture, perhaps also linked to a small phreatomagmatic structure about two hundred metres in diameter.

On the Awash left bank, 500 metres south of the confluence of the Atebella and Balchit gullies, a rounded structure about 300 metres in diameter can be seen, probably an ancient lake infill of an aphyric fluidal lava (Fig. 3). This is very similar to the lava of the fault system bordering Melka Kunture in the South.

The lavas corresponding to the magma that originate with this vulcanism mainly appear along the faulted zone with intrusive aspects revealed by their jointed orientation or in flow onset organisation. We also note the presence of basaltic doleritic lavas, with spectacular porphyric facies (sample 2161), set in breccias or as inclusions in ignimbrites. Actually, the flow dynamics seem to have been influenced by the presence of water, indicated by the presence of typical phreatomagmatic breccias (diatreme facies), vesicular tuffs (sample 2052) with surges figures, and lapillis falls with yellowish cement. These grade into a more purely strombolian projection facies with scorias, bombs, etc. (Fig. 4). The microscopic characters of these facies were identified in two localities and are now described.

Fig. 3. Lava lake structure 500 m downstream from Atebella and Balchit Creeks confluence. *Cliché J.-P. Raynal*

Fig. 5. Doleritic porphyric lava at Wutale East Gully: A, natural light; B, polarized light. *Cliché G. Kieffer*

Fig. 4. Strombolian bomb at Godeti. *Cliché G. Kieffer*

Wutale East Gully (sample 2161): Doleritic porphyric and vesicular lava with large plagioclase crystals (up to 1 cm; Fig. 5A, B). We also observed some augites and abundant olivine. The black coloured groundmass is feebly crystallised and oxidised. A rust coloured alteration is visible on the vesicle walls, as well as yellow mineral deposits. This basaltic rock comes from the scoriated zone of a flow or of another laval mass.

Awash Crossing (sample 2052): In the lower third of the thin section, a laminated mixture of broken minerals and fragments of various lavas is visible in

an argilo-clastic matrix that also contains a few scoria or vesicular pumice fragments. These latter are oxidised black and altered and affected by a diffuse alteration also visible in the matrix. Also evident are vesicles of different sizes, richer in some beds than in others. We also find phreatic surges and very fine example of vesicular tuffs (Fig. 6).

In the two upper thirds of the thin section, the elements are coarser with many scoriated fragments (black or very dark). In the whole example the matrix is less abundant, and more or less represented according to its position within the units. Inter-granular voids are present as well as vesicular surges of phreatomagmatic origin.

It should be noted that the landforms of this initial activity have been truncated and levelled by erosion so that they do not by themselves determine any former topographical relief (that is to say apart from later tectonic events which could have affected them). This indicates a long morphological evolution and thus, a rather great age. We suggest that this activity could be contemporaneous with the Guraghe basalts, between 8.3 and 10.6 Ma (Woldegabriel *et al.* 1990).

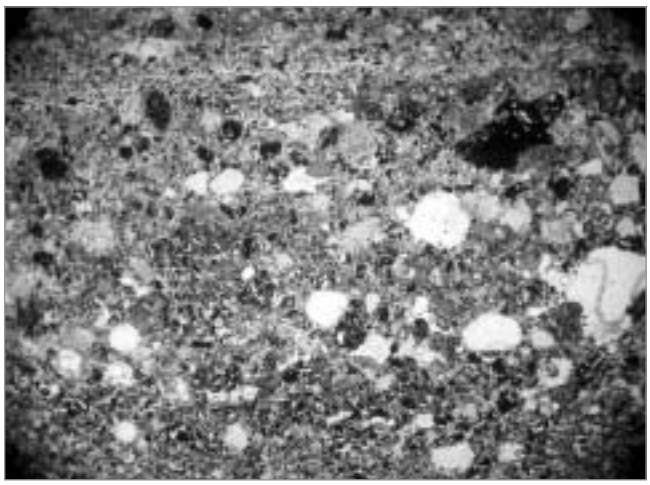

Fig. 6. Vesiculat tuffs at Awash crossing; natural light. *Cliché G. Kieffer*

Fig. 7. Wachacha trachytic domes. *Cliché J.-P. Raynal*

The intermediary activity

With very differentiated magmas, particularly rhyollites, this activity was mainly explosive and is the origin of a wide variety and considerable volume of pyroclastites.

They followed the basaltic eruptions that continued around 8 Ma (Mohr 1999).

This may be less than 4 or 5 Ma old. It occurred in several phases, some of them perhaps contemporaneous with several other volcanoes present in the Melka Kunture environment, for example in the north the Wachacha (Fig. 7), Gara Furi or Yerer whose trachytic products are dated to 3.1 and 4.4 Ma (Chernet *et al.* 1998); or in the south the ignimbrite from Butajira dated from 3 to 4.2 Ma or the trachyte from Chilalo at between 1.6 and 3.5 Ma (Woldegabriel *et al.* 1990). The number of ignimbrite facies, welded or non-welded (twenty at least), visible *in situ* or reworked into ancient or recent alluviums of the Melka Kunture area and its environment, indicates the multiplicity of eruptive phases which marked the region.

Fig. 8. Troglodytic settlement excavated in pyroclatic flows near Roge. *Cliché J.-P. Raynal*

Fig. 9. Troglodytic church excavated in ignimbrite at Adadi Mariam. *Cliché J.-P. Raynal*

Fig. 10. Welded ignimbrite with columnar jointing at Gobu, foothill of Wachacha (in background). *Cliché J.-P. Raynal*

Pyroclastic flows and the pilling of direct or reworked falls, become more numerous and thicker proceeding towards the southwest. An interesting feature in the upstream part of the Simbiro gully, around the Roge plateau and towards Adadi Mariam, are the troglodytic settlement and sanctuaries, completely excavated in the ignimbrites (Figs. 8, 9). So, the probable origin of most of these manifestations could be more than 20 kilometres away in the Werebo Chancho block or at the end of the Guraghe Mounts whose altitude reaches or passes 3000 metres.

During an eruptive phase, dated to 4.37 Ma (Chernet *et al.* 1998), the small block of rhyolitic obsidian was produced at Balchit, a few kilometres north of Melka Kunture. It is probably a flow or dome-flow structure that barely contributes specific relief to the area, but the importance of which comes from its long utilization for artefact manufacture, particularly bifaces which are very well represented in prehistoric sites.

The welded ignimbrites

Some important eruptive episodes deposited welded ignimbrites. These formations, whose precise origin still remains to be determined, can be correlated with ignimbrites attributed to the Wachacha ("Balchi Rhyolites") and dated of 4.5 Ma or to others visible in the Akaki canyon and dated at 5.2 Ma (Justin-Visentin *et al.* 1975).

It is possible to distinguish successive facies in the eruptive chronology, one with fiamme and one without fiamme.

The ignimbrite with fiamme exhibits clear prismatic structure. The obsidian rich fiamme are up to several centimetres thick and their length (extension in the flattened plane) is sometimes over ten centimetres. Other ignimbrites having a greyish groundmass appear lavic, are rich in quartz and feldspath crystals.

Welded ignimbrites lacking fiamme, are regionally common and show a lavic facies that could have been previously mixed with true lava. It is generally well prismed (Figs. 10; 11A, B; 12) with occasionally a basal obsidianic bedsole a few decimetres thick. Like the ignimbrite with fiamme, it shows a vitreous fluidal texture with vitroclastic, porphyry, with abundant quartz and feldspar crystals.

Several localities from the south slope of the Wachacha to the south of Melka Kunture were examined to determine micro-facies.

Gobu (sample 2032): Fluidal very porphyric vitreous structure. Continuous vitreous groundmass of the rock with fine figures of fluidality. Rather light brown glass. Vacuoles stretched and elongated by the rock fluidality. Abundance (>50%) of potassic feldspars and quartz crystals, from automorphic phe-

Fig. 11. Atebella Creek. A, welded ignimbrite at Atebella forming threshold. B, prism of welded ignimbrite with cooling features. *Cliché J.-P. Raynal*

Fig. 12. Tinishu-Kersa, non-welded ignimbrite overlaying welded ignimbrite with large columnar jointing.
Cliché J.-P. Raynal

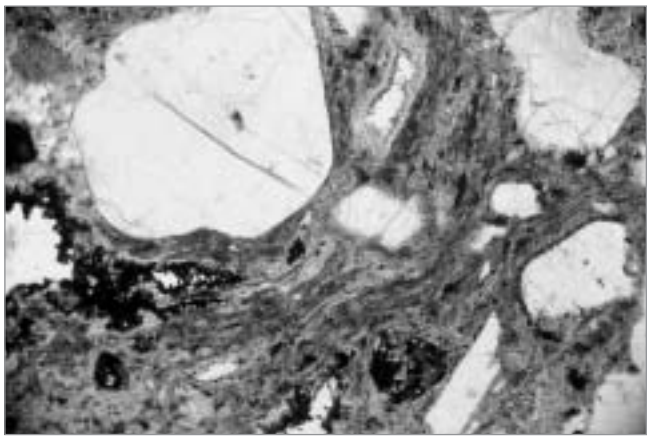

Fig. 13. Tinishu-Kersa, microstructure of welded ignimbrite; microscopic view in natural light.
Cliché G. Kieffer

nocrystals (>1 mm) to all sizes fragments, smaller, in flake crystals. Two lava fragments. A vesicular inclusion. Alteration in opaque impregnations.

Alemgana Quarry (sample 9907): Similar to 9904 and 9905, with a vitroclastic tendency rather more marked, the glass slightly less abundant, large altered vesicular pumices with recrystallisation as already noted. Green denticulated augite present. Very fine devitrification (small dots visible under polarised light) is present in the glass, as for 9901 of Tinishu-Kersa.

Tinishu-Kersa (sample 9901): Vitreous fluidal structure, very finely recrystallized (or altered), porphyric structure with rather abundant sub-automorphic alkaline feldspars, minute fragments of the latter are cemented into the glass, remains of large vesicular and stretched pumices, of very weathered ferro-magnesians hard to identify (biotite, or brown hornblende). Recrystallisation takes place in the voids left by original bubbles or pumices destroyed by alteration or weathered minerals, with in some cases a border of well crystallised bubbles and the inside apparently occupied by zeolites (?). Glass ≥ 50%. Rock very weathered. Opacity may be due to alteration residues? (Fig. 13).

Simbiro Ford (sample 9904): Vitreous fluidal structure with a vitroclastic tendency (glass ≥ 50% of the rock). The fluidality of the glass follows the minerals. A few big vesicular altered pumices, a lot of alkaline sub-automorphic feldspar phenocrystals with many smaller and variously sized fragments (as for 9901). Very rare ferro-magnesium compounds (3 or 4 in the thin section); very weathered brown (hornblende?). Considerable alteration, thin bands of recrystallisations present in the biggest weathered pumices (as for 9901; tridymite or cristoballite? zeolites?), rusty red to black alteration products.

Atebella Ford (sample 9905): As for 9904 but the crystals of alkaline feldspars are more abundant, glass perhaps a little less abundant (= 50%), greater frequency of large altered vesicular pumices. Important alteration, recrystallisation of vesicles (perhaps having a calcite edge?).

Melka Garba, left bank (sample 9909): Vitreous structure poorly vitroclastic, rather fluidal, glass brown to blackish-brown, coarse fragments of fibrous or vesicular pumices present (altered), relatively high proportion of alkaline feldspars in sub-automorphic phenocrystals or in fragments of various sizes. High degree of alteration and recrystallisation.

The two facies of welded ignimbrites belong to distinct eruptive phases. They were preceded, separated and followed by numerous manifestations at the origin of pyroclastic ashy-pumiceous flows and of pumice and ash fallouts, particularly emitted by powerful plinian or phreato-plinian eruptions. Two sections show the relationship of the various formations to these ignimbrites:

Section upstream of the Simbiro Creek described from bottom to top:

- products belonging to the initial basic or benmoreitic vulcanism,
- several tuff types with a phreato-magmatic bed at least 2 or 3 metres thick,
- a unit of ignimbrite with fiamme forming a well developed surface constituting the major bed of the creek. Laterally, a thick lag-fall unit could possibly preceed the ignimbrite itself (Fig. 14),
- a decimetric to metric horizon in which some pedogenesis took place,
- an ashy-pumiceous flow, non-welded, three to four metres thick,
- stratified tuffs, of plinian or phreato-plinian origin,
- ignimbrites without fiamme,
- white and yellowish stratified tuffs.

Fig. 14. Simbiro Creek upstream. Thick lag-fall unit below several ignimbrites and phreato-plinian deposits. *Cliché J.-P. Raynal*

Double waterfall in the upstream course of the Wutale Creek, section described from bottom to top:

- several tuffaceous units (direct or reworked fine pumiceous fallouts),
- ignimbrite with fiamme divisible into three units (Fig. 15):
  - a lag-fall from one to three metres thick, constituting the base of the whole. This rocky unit is made of loose lavic elements that can reach ten centimetres in diameter (basalt: 45%; differentiated porphyric rocks: 33%; differentiated aphyric to subaphyric: 12%; trachy-basalts: 8% and various: 2% with feldspathic inclusions and an indeterminate ignimbrite),
  - an intermediate unit one to two metres thick corresponding to a consolidated breccia, with the same composition as the previously described lag-fall unit,
  - a three to five metre thick unit of massive prismatic ignimbrite, that seems to have caused some ravine development in the underlying loose or consolidated units of the lag-fall when it set;
- several tuff beds (phreato-magmatic, ignimbrites, phreato-plinian),
- a unit of welded ignimbrite without fiamme, massive and prismatic a few metres thick.

Fig. 15. Wutale Creek. The three units of the ignimbrite with fiamme. From bottom to top: lag-fall, breccia, massive ignimbrite. *Cliché G. Kieffer*

It is probable that significant reactivation of the Melka fault took place after this episode because the welded ignimbrite only remains as small nappe outliers on the slope created by the play of the varied accidental segments. In addition, it can be seen that erosion cut and raised it into prominence before the deposition of the later products.

The post-welded ignimbrites activity

The first products of the later events generally correspond to pumice falls. Among them, we can distinguish a powerful phreato-plinian series. Later volcanic episodes mainly consist of distal deposits, tuffs and plinian falls, interstratifying in the mainly volcano-detritic sedimentation of the basin. These are found again in the old series of Gombore and Garba in particular (Fig. 16). This activity is interspersed with phreatomagmatic episodes, of which some outliers remain as ashy beds with specific characteristics.

In the series of Gombore and Garba, the volcanic input is of course very important in most of the deposits and several beds had previously been described as tuffs, but we reserve the term tuff for the units which are in primary to subprimary position. We have identified these tuff units, described them in thin sections, established their geochemistry and defined the volcanic dynamic responsible for their emission. When this was possible, we have taken into account previous geochemical and palaeomagnetic data as well as K/Ar datings (Taieb 1974; Schmitt *et al.* 1977; Cressier 1980). We chose to temporarily label the tuff units after the sample numbers, avoiding therefore the problem of premature correlations on the basis of a lettering system as it was previously used on theses sites (Schmitt *et al.* 1977; Chavaillon 1979c; Cressier 1980).

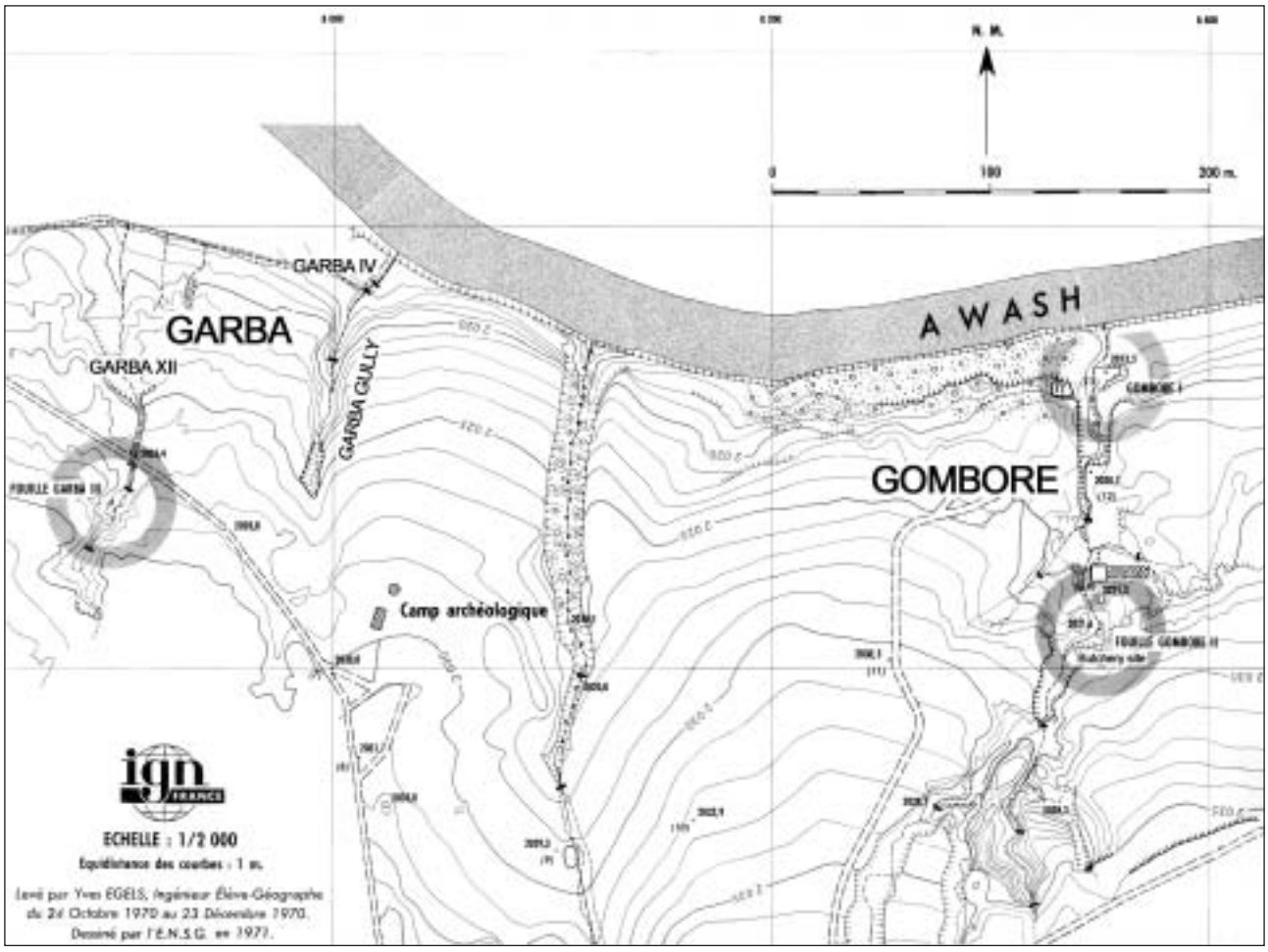

Fig. 16. Detailed map of the Gombore-Garba sectors (after Egels 1971).

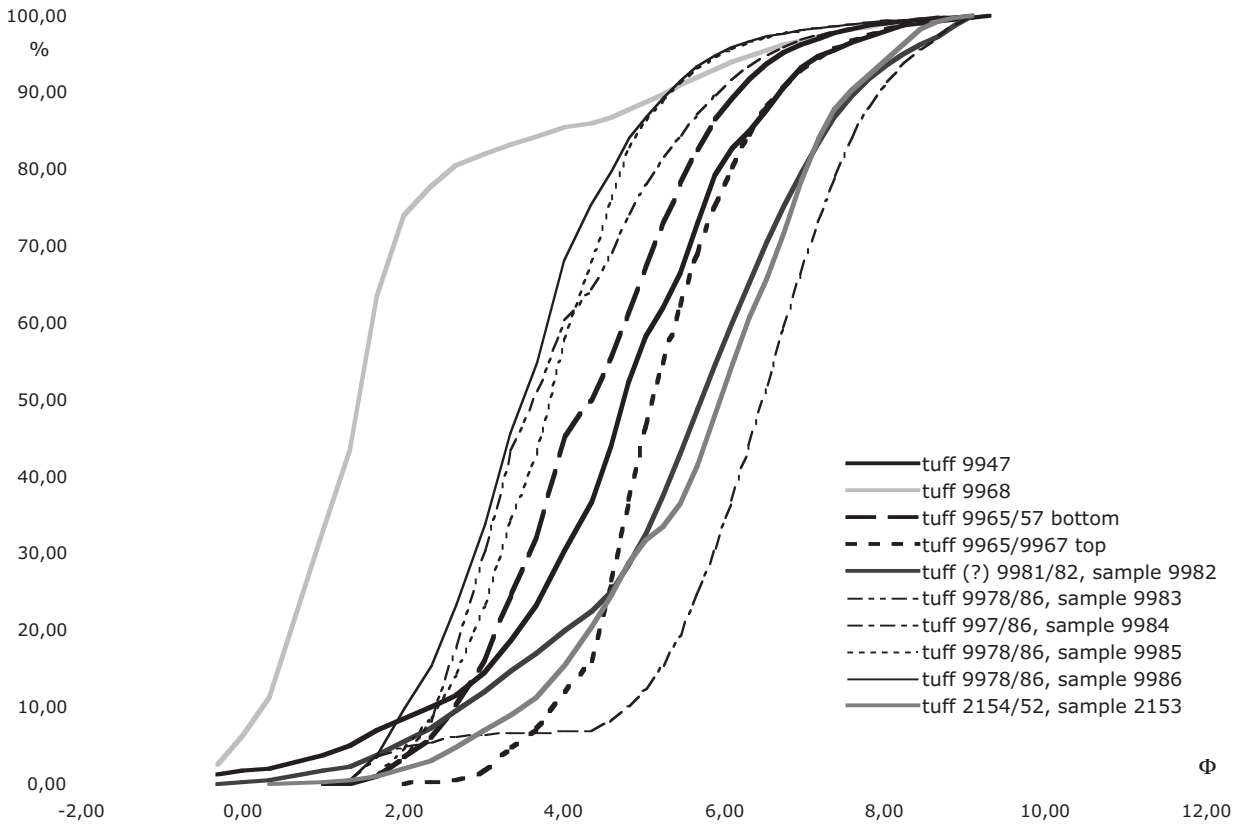

Fig. 17. Granulometry of tephras at Gombore I.

Tuffs of the Gombore I series

From the bottom of the Gombore I section to the top of Gombore II "Butchery site", several tuffs have been identified in primary to subprimary position.

Tuff 9945/47: This tuff unit was sampled by J. Chavaillon during his excavations at Gombore I between archaeological Layers B2 and B3. This silty-sandy tephric unit is well sorted (Fig. 17) and its Inman (1952) parameters (Md_{Φ} = 4.75 and σ_{Φ} = 1.55) place it in the "fall" field of the Md_{Φ}/σ_{Φ} diagram (Walker 1971; Walker and James 1992). In thin section, it is a very fine massive pelitic unit without visible stratification. A few white minerals (quartz and feldspars) can be distinguished along with numerous more or less homo-metric small pumices. Concentrations of black oxides occur in patches more or less star shaped (1 mm). Sediment is rich in pumices (direct fall or concentration of sorted pumices?) piled up in a muddy form because of a pelitic matrix. Geochemistry indicates a rhyolitic magma and an elementary composition quasi-identical to the "Grazia tuff" at the bottom of the Garba IV series (Tab. 1). Polarity of the tuff itself has not been established but units below and above are considered as reverse (Cressier 1980).

Tuff 9968: This sandy tephric unit is well sorted (Fig. 17) and its Inman (1952) parameters (Md_{Φ} = 1.45 and σ_{Φ} = 1.52) place it in the "fall" field of the Md_{Φ}/σ_{Φ} diagram (Walker 1971). Geochemistry indicates a dacitic magma. It's position is identical to the tuffaceous lense of reverse polarity sampled by Jaeger 0.15 m above the Gombore Iγ archaeological layer (Cressier 1980).

Tuff 9965/67: The bottom is a well sorted silty-sand (Fig. 17) and its Inman (1952) parameters (Md_{Φ} = 4.35 and σ_{Φ} = 1.37) place it in the "fall" field of the Md_{Φ}/σ_{Φ} diagram (Walker 1971). In thin sec-

	SAMPLES	TUFFS IN GOMBORE AND GARBA SERIES																									NON-WELDED IGNIMB.		
		9915	9920	9922	9923	9924	9938	9943	9944	9947	9948	9949	9959	9962	9966	9967	9968	9977	9983	9984	9985	9986	9989	2151	2152	2153	2155	2156	2157	9910	236	142
TRACE ELEMENTS	As ppm	1,53		1,68			3,98	1,40	2,10	1,62	1,78					2,77	0,82		1,70	1,52			3,02	0,99	1,44	1,79	1,95			1,98		
	Ba ppm	120,90		526,70			95,57	1671,00	1571,00	549,80	161,90					498,60	759,90		668,80	670,60			512,50	369,30	693,50	980,40	497,30			643,50		
	Be ppm	5,91		5,64			7,71	4,65	7,70	5,71	5,74					5,74	2,64		4,49	4,53			5,95	5,17	4,82	4,56	6,31			5,13		
	Bi ppm	0,11		0,10			0,21	0,12	0,10	0,14	0,11					0,09	< L.D.		0,08	0,08			0,13	0,14	0,09	0,09	0,12			0,07		
	Cd ppm	0,95		0,97			1,17	0,76	1,07	0,94	1,14					0,82	< L.D.		0,94	1,20			0,60	0,65	0,75	0,46	0,60			1,07		
	Ce ppm	243,70		205,30			214,00	212,00	220,80	211,80	224,40					160,70	192,50		198,30	194,60			206,00	194,80	195,50	154,10	225,60			194,10		
	Co ppm	12,06		3,39			1,27	8,44	4,74	6,11	17,64					6,92	15,70		6,11	5,84			3,54	12,74	5,29	0,48	3,41			2,08		
	Cr ppm	9,14		8,54			6,64	< L.D.	6,89	14,60	9,59					5,92	30,01		9,26	7,54			6,70	45,21	< L.D.	5,69	5,61			6,22		
	Cs ppm	1,07		1,09			1,79	0,99	2,45	1,07	1,02					1,25	1,29		1,33	1,78			1,71	2,31	1,79	1,49	1,78			0,81		
	Cu ppm	11,12		10,55			6,40	11,46	9,87	13,40	9,51					10,26	20,41		8,58	9,58			7,91	17,93	4,75	6,04	7,00			7,58		
	Dy ppm	21,94		18,62			22,04	8,71	14,73	18,95	17,99					14,52	13,22		16,07	16,85			16,84	15,18	15,79	11,10	18,70			17,37		
	Er ppm	12,69		10,07			12,93	5,02	8,66	10,33	10,09					8,77	7,05		8,82	9,38			9,95	8,92	8,71	6,22	10,73			9,52		
	Eu ppm	3,44		4,11			1,36	1,01	1,06	4,29	3,01					2,96	4,05		3,60	3,83			1,68	2,28	3,65	3,49	2,04			3,74		
	Ga ppm	29,94		32,19			31,30	39,39	34,00	33,37	30,01					30,45	24,94		28,04	28,33			33,11	28,76	28,05	25,66	33,43			33,33		
	Gd ppm	21,32		18,61			19,68	8,90	13,76	19,08	18,10					13,42	14,34		16,24	16,96			15,82	14,95	16,23	11,51	18,18			17,54		
	Ge ppm	2,37		2,40			2,91	2,32	2,55	2,49	2,19					2,53	1,76		2,49	2,42			2,25	2,17	2,37	1,77	2,22			2,40		
	Hf ppm	22,45		22,33			33,32	24,48	20,92	22,27	22,01					16,69	7,84		18,83	18,66			20,81	17,79	18,93	13,78	20,36			20,05		
	Ho ppm	4,44		3,60			4,41	1,73	2,93	3,65	3,52					2,98	2,52		3,10	3,27			3,40	3,09	3,07	2,16	3,73			3,39		
	In ppm	0,21		0,24			0,22	0,18	0,18	0,24	0,22					0,22	0,10		0,21	0,21			0,25	0,13	0,18	0,12	0,16			0,23		
	La ppm	132,70		95,66			99,99	68,04	125,90	100,00	113,40					74,81	97,11		91,07	93,82			105,40	108,60	91,12	75,83	122,10			92,94		
	Lu ppm	1,99		1,53			2,08	0,81	1,42	1,53	1,52					1,42	0,97		1,33	1,40			1,54	1,48	1,33	1,00	1,64			1,48		
	Mo ppm	5,37		5,64			10,43	2,05	6,85	5,17	6,80					4,45	1,16		4,10	3,71			4,60	2,25	3,74	3,82	3,34			6,80		
	Nb ppm	103,50		100,10			176,60	212,10	199,80	103,00	100,40					100,90	43,99		91,03	90,10			132,30	126,00	91,37	82,12	132,60			96,16		
	Nd ppm	113,50		95,10			94,34	52,34	83,95	99,65	100,20					66,76	87,82		92,44	95,70			87,93	84,87	91,77	67,79	102,90			91,70		
	Ni ppm	10,24		6,01			< L.D.	14,95	< L.D.	13,76	10,30					6,91	15,92		6,80	6,66			6,73	22,37	6,15	< L.D.	5,72			< L.D.		
	Pb ppm	16,25		15,81			25,70	23,13	20,03	16,12	15,78					12,61	9,99		13,81	13,43			22,72	19,52	12,59	13,92	21,95			14,18		
	Pr ppm	29,96		24,43			25,36	14,87	24,41	25,52	26,62					17,66	22,97		23,66	24,52			24,06	23,51	23,66	18,04	28,23			23,60		
	Rb ppm	118,10		121,90			173,10	79,33	189,60	99,52	131,20					159,10	66,71		105,00	139,30			149,80	106,20	126,40	85,08	154,30			87,65		
	Sb ppm	< L.D.		< L.D.			< L.D.	< L.D.	< L.D.	< L.D.	< L.D.					< L.D.	< L.D.		< L.D.	< L.D.			0,33	0,22	0,26	0,20	0,27			< L.D.		
	Sm ppm	23,12		20,51			21,25	10,19	15,97	21,21	20,34					14,20	16,93		18,78	19,52			17,77	16,79	18,60	13,31	20,71			19,53		
	Sn ppm	7,12		7,28			9,91	7,85	6,86	7,44	6,83					5,21	2,40		5,76	5,64			6,24	5,05	5,44	3,90	6,33			6,42		
	Sr ppm	30,26		32,07			18,75	78,78	54,91	24,15	46,26					43,22	210,10		75,64	101,00			58,23	115,30	79,61	118,70	60,84			51,20		
	Ta ppm	8,28		7,76			12,88	16,58	14,22	7,79	8,26					7,38	3,22		6,69	6,57			10,65	9,25	6,48	5,85	10,42			7,20		
	Tb ppm	3,53		3,06			3,46	1,47	2,34	3,14	3,00					2,32	2,26		2,68	2,81			2,69	2,48	2,64	1,85	3,03			2,89		
	Th ppm	14,86		13,16			25,34	29,05	23,64	13,91	14,75					10,72	6,26		10,65	10,67			19,67	18,51	10,84	10,74	19,79			11,52		
	Tm ppm	1,92		1,50			2,00	0,81	1,34	1,52	1,52					1,35	1,02		1,32	1,37			1,52	1,38	1,31	0,97	1,65			1,43		
	U ppm	5,97		3,44			6,96	2,56	5,55	3,44	5,79					3,05	2,30		3,16	3,06			7,02	3,24	2,99	2,76	5,93			6,92		
	V ppm	32,57		11,75			10,66	24,19	11,91	24,14	109,00					20,53	34,24		47,11	31,91			20,72	56,72	27,09	5,62	17,32			16,49		
	W ppm	1,55		1,92			3,43	1,67	2,72	1,99	1,84					1,65	1,20		1,32	1,21			2,08	1,91	1,36	1,47	2,17			1,62		
	Y ppm	140,20		102,90			131,40	46,46	84,60	104,00	103,40					85,34	73,40		87,33	94,66			97,77	88,19	91,04	64,76	109,60			97,79		
	Yb ppm	12,90		10,05			13,57	5,50	9,23	10,17	10,11					9,26	6,68		8,71	9,18			10,21	9,67	8,76	6,57	11,06			9,61		
	Zn ppm	189,80		222,10			221,80	126,10	178,10	224,70	194,30					209,30	91,62		182,90	184,10			157,30	139,90	175,30	115,50	167,50			224,50		
	Zr ppm	947,90		931,10			1334,00	1193,00	969,10	936,40	931,00					718,80	332,10		820,50	823,60			891,20	847,70	889,50	641,40	888,30			848,00		
MAJOR ELEMENTS	SiO2 %	67,20	67,40	70,43	64,50	63,24	70,59	54,19	60,24	67,43	67,19	63,81	60,93	64,04	65,41	61,88	65,43	61,21	67,19	68,51	64,91	65,84	64,70	59,57	68,07	65,61	66,03	62,55	62,18	68,40	67,95	65,90
	Al2O3 %	9,68	10,88	9,98	13,32	9,93	10,64	17,29	14,21	9,63	10,87	11,83	13,86	15,89	10,70	11,23	14,26	15,72	10,81	10,85	10,83	10,85	13,74	14,96	11,01	15,19	13,81	13,63	13,56	10,08	11,20	11,25
	Fe2O3 %	5,54	5,68	4,80	5,56	8,72	3,48	8,69	7,02	5,77	5,47	6,20	6,21	4,33	7,54	7,93	4,63	5,89	5,23	5,10	6,33	5,80	4,51	5,79	4,92	2,91	4,36	5,64	5,79	5,94	5,80	6,50
	MnO %	0,20	0,15	0,17	0,10	0,19	0,18	0,23	0,20	0,61	0,15	0,16	0,07	0,09	0,33	0,32	0,07	0,07	0,19	0,15	0,16	0,16	0,07	0,10	0,14	0,16	0,07	0,06	0,05	0,17	0,15	0,15
	MgO %	0,32	0,37	0,24	0,56	0,57	0,25	0,50	0,40	0,38	0,45	0,60	0,71	0,41	0,27	0,41	0,57	0,66	0,46	0,40	0,77	0,56	0,26	0,72	0,40	0,54	0,35	0,80	0,72	0,40	1,35	1,25
	CaO %	1,30	0,64	0,38	1,19	1,23	0,19	1,16	0,87	1,00	0,51	0,79	1,28	1,34	0,61	0,81	1,67	1,60	0,97	0,93	1,60	1,17	0,81	1,43	0,95	1,03	0,84	1,31	1,38	0,99	0,70	0,50
	Na2O %	1,59	1,58	1,17	3,16	1,16	2,12	2,34	2,24	1,51	2,54	1,93	2,46	4,43	1,51	0,96	3,67	3,21	1,94	1,06	1,96	1,89	3,21	2,20	1,51	3,22	3,09	2,16	2,29	3,75	3,75	3,15
	K2O %	4,54	4,34	5,41	3,58	3,37	5,19	2,51	4,27	4,53	4,53	3,77	2,45	3,49	4,81	4,24	3,18	2,77	4,60	4,37	4,02	4,18	4,25	2,46	4,21	4,64	4,32	2,19	2,20	4,98	4,00	4,05
	N+K	6,13	5,92	6,58	6,74	4,53	7,31	4,85	6,51	6,04	7,07	5,70	4,91	7,92	6,32	5,20	6,85	5,98	6,54	5,43	5,98	6,07	7,46	4,66	5,72	7,86	7,41	4,35	4,49	8,73	7,75	7,20
	TiO2 %	0,31	0,62	0,30	1,17	0,56	0,21	0,43	0,33	0,35	0,38	0,52	1,09	0,89	0,49	0,72	0,64	1,42	0,66	0,53	1,03	0,90	0,39	0,95	0,57	0,55	0,40	1,06	1,10	0,48	0,60	0,50
	P2O5 %	0,47	0,05	< L.D.	0,10	0,20	< L.D.	0,08	0,07	0,31	< L.D.	0,09	0,10	0,11	0,07	0,12	0,15	0,17	0,11	0,12	0,16	0,11	0,06	0,14	0,09	0,13	0,10	0,13	0,11	0,17	0,15	0,10
	PF %	8,12	8,22	6,90	6,68	10,72	5,88	12,75	10,11	8,37	7,82	9,81	10,74	4,90	8,68	10,21	5,65	7,21	7,77	7,90	8,17	8,49	7,03	11,59	8,36	5,56	6,93	10,37	10,52	4,60	4,20	5,90
	Total %	99,27	99,93	99,78	99,92	99,89	98,73	100,17	99,96	99,89	99,91	99,51	99,90	99,92	100,42	98,83	99,92	99,93	99,93	99,92	99,94	99,95	99,03	99,91	100,23	99,54	100,30	99,90	99,90	99,96	99,85	99,25

Tab. 1. Geochemistry of Melka tephras. Major elements normalized to 100% anhydrous and reported in weight. Trace elements in ppm. Samples 236 and 142 after Taieb (1974).

tion, it is a microconglomerate first lacking matrix, but gradually becoming richer. Abundant subautomorphic feldspathic elements and fragments of fibrous and vesicular pumice. Alteration evident, particularly in the calcite edges around the components. The upper part shows a transition to a thinner sequence made of glass splinters with a few automorphic microlites mainly feldspathic (Fig. 18). A felted aspect of and appearance of pseudo-fluidality is given by the disposition in the beds of the pumices fibres aligned according to their plane of elongation. A few variations in the size of elements (smaller towards the top) but same vitreous composition as seen in the lower part. The differences in the size of the elements from one bed to another emphasise the stratification that is present. Whole provides evidence of a direct distal fall with blown pumices. Geochemistry indicates a rhyolitic magma.

The top part is a very well sorted silty bed (Fig. 17) half a centimetre thick and its Inman (1952) parameters (Md_Φ = 5.10 and σ_Φ = 0.95) place it in the "fall" field of the Md_Φ/σ_Φ diagram (Walker 1971). In thin section, it appears rich in thin crystal fragments of various natures (Fig. 19). These are highly altered which is typical of a distal phreatomagmatic fallout. Geochemistry indicates a dacitic magma. The position of this tuff unit is identical to the tuffaceous layer of reverse polarity sampled by Jaeger 0.85 m above the Gombore Iγ archaeological layer (Cressier 1980; Fig. 20).

Tuff (?) 9981/82: This unit caps the section at Gombore Iγ (Fig. 20). It is made of well sorted sandy silt (Fig. 17) and its Inman (1952) parameters (Md_Φ = 4.20/5.70 and σ_Φ = 1.77/1.85) place it in the "fall" field of the Md_Φ/σ_Φ diagram (Walker 1971). We consider this unit as reworked tuffs and have not investigated it in thin section nor established its geochemistry.

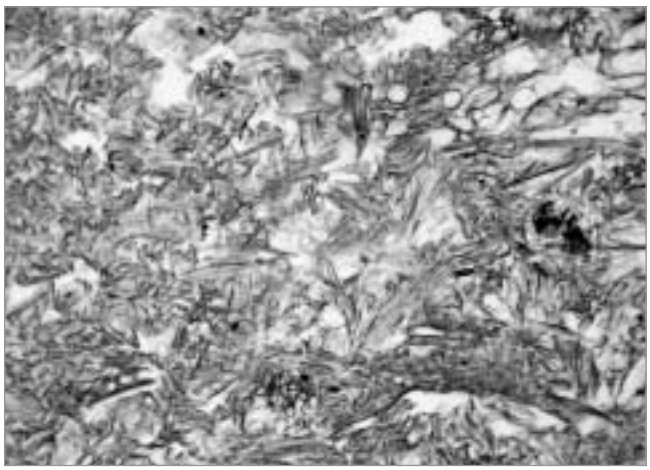

Fig. 18. Gombore I, tuff 9965/67, bottom part; microscopic view in natural light. *Cliché G. Kieffer*

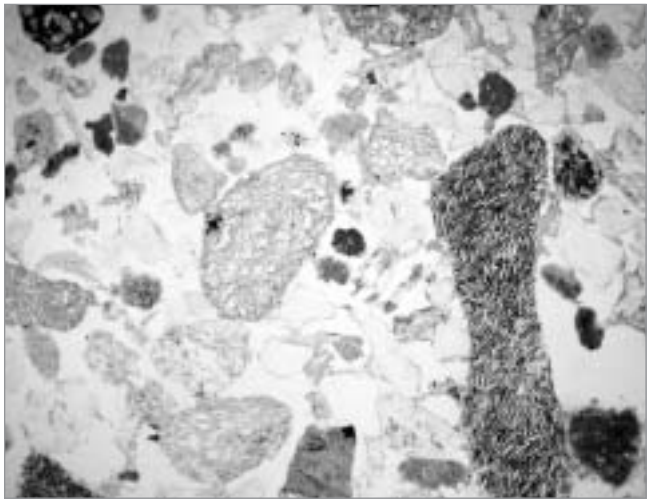

Fig. 19. Gombore I, tuff 9965/67, top part; microscopic view in natural light. *Cliché G. Kieffer*

Fig. 20. Gombore Iγ section with tuff (?) 9981/82 at top. *Cliché J.-P. Raynal*

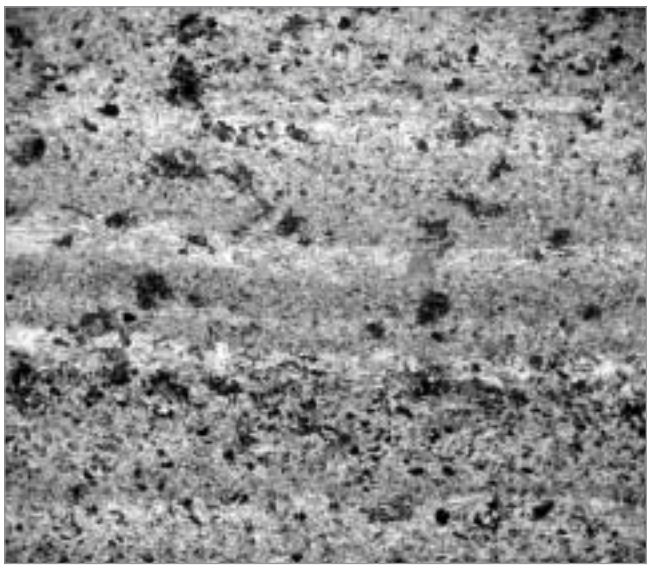

Fig. 21. Gombore I, Tuff 9978/86, bottom part (sample 9978); microscopic view in natural light. *Cliché G. Kieffer*

Fig. 22. Gombore I, Tuff 9978/86, middle part with circumvolutions (sample 9987); microscopic view in natural light. *Cliché G. Kieffer*

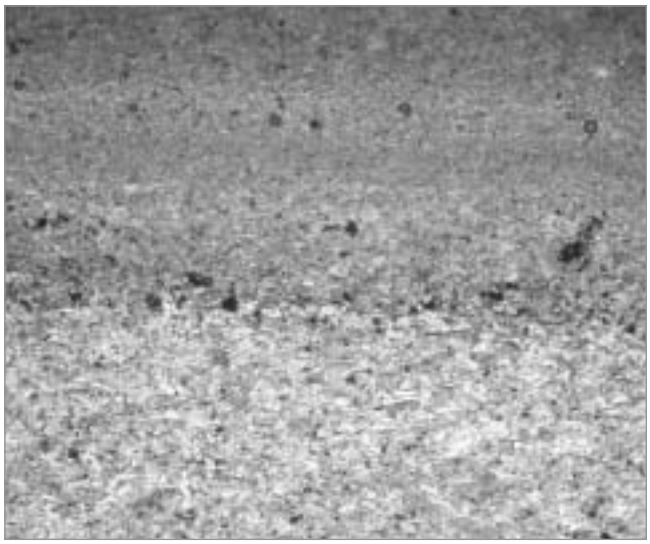

Fig. 23. Gombore I, Tuff 9978/86, middle part (sample 9987); microscopic view of finest laminae in natural light. *Cliché G. Kieffer*

Tuff 9978/86: The stratigraphic status of this tuff unit is still in debate. Despite several test pits and trenches, we never could clearly establish wether or not this tuff unit, which overlies the Gombore I succession, precedes the Gombore II channel accumulation and several hypotheses should be considered. This tuff unit is nearly 1.00 m thick and has been identified previously as reverse "tuff B" (Chavaillon 1979c; Westphal *et al.* 1979; Cressier 1980), but no paleomagnetic data nor absolute dating was produced for the Gombore I outcrop. From the bottom to the top, several samples have been analysed which have different granulometry and content:

Samples 83/84/78: Sample 9983 is a well sorted silty sand (Fig. 17) and its Inman (1952) parameters (Md_Φ = 3.61 and σ_Φ = 1.40) place it in the "fall" field of the Md_Φ/σ_Φ diagram (Walker 1971). Its geochemistry indicates a rhyolitic magma. Sample 9984 is a well sorted sandy silt (Fig. 17) and its Inman (1952) parameters (Md_Φ = 6.47 and σ_Φ = 1.20) place it in the "fall" field of the Md_Φ/σ_Φ diagram (Walker 1971). Its geochemistry indicates a rhyolitic magma. In a thin section (sample 9978), we see a fine to pelitic sequence with very distinct stratification (Fig. 21). Lower part of fine to very fine felt with glass splinters and a few feldspars, the whole weathered. This is evidence of a more or less distal direct fall. In the medial part of the thin section, which is about 3.5 cm thick, a more varied mixture occurs with abundant ochre and opaque elements and some feldspars. This may be a distal phreatomagmatic fall.

Sample 9985: This is a well sorted silty sand (Fig. 17) and its Inman (1952) parameters (Md_Φ = 3.81 and σ_Φ = 1.07) place it in the "fall" field of the Md_Φ/σ_Φ diagram (Walker 1971). Its geochemistry indicates a dacitic almost rhyolitic magma.

Sample 9987: In thin section, this shows a very fine to pelitic sequence in the middle and at the top, but in the central portion there are variations in thickness with circumvolutions (Fig. 22). In the finest laminae (Fig. 23), splinters or very fine

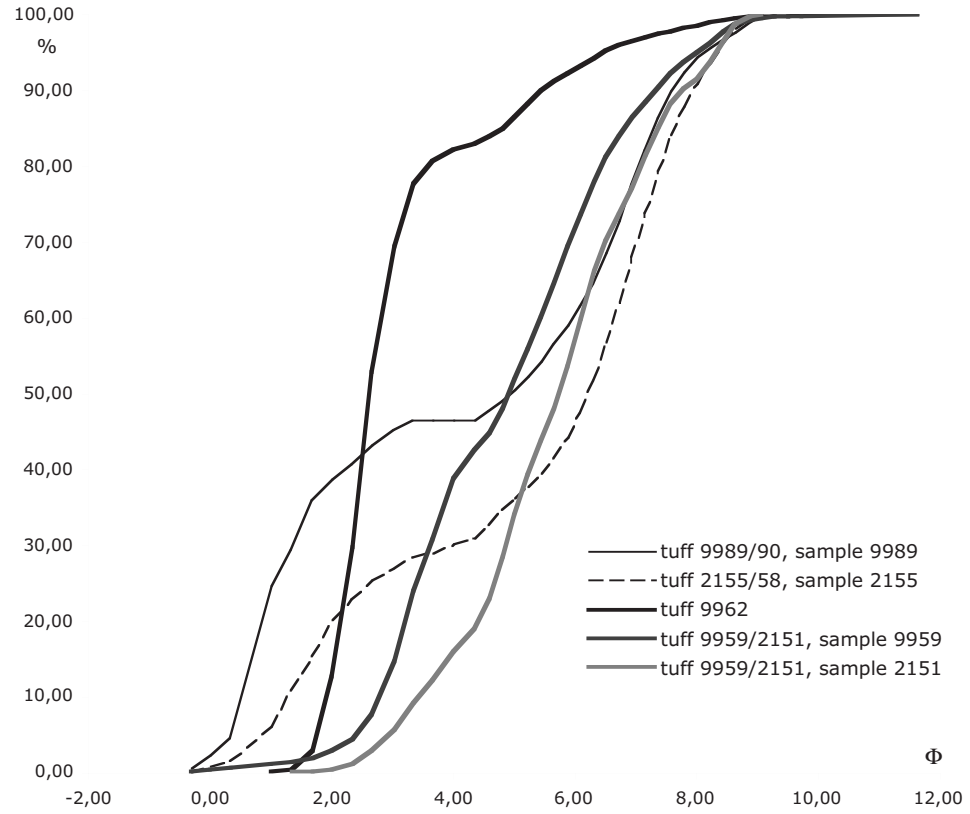

Fig. 24. Granulometry of Gombore II tephras.

rods of fibrous glass are present. Some very fine feldspar fragments and other black or ochre-rust altered elements can be seen. This is a direct distal fall.

Sample 9986: This is a well sorted silty sand (Fig. 17) and its Inman (1952) parameters (Md_{Φ} = 3.49 and σ_{Φ} = 1.22) place it in the "fall" field of the Md_{Φ}/σ_{Φ} diagram (Walker 1971). Its geochemistry indicates a rhyolitic magma (Tab. 1).

Tuff 2154/52: This tuff constitutes the southern outcrop of tuffs described *supra* (samples 9978 to 9986).

In thin section, we have at the base (2154) a few minerals (quartz and feldspaths) added to the pumices fragments mainly as glass splinters and a few oxidised fragments and various lavas. The main part of the thin section is mostly composed of dispersed glass splinters. The pseudo-stratification probably indicates a surge linked to a rather distant plinian eruption.

The top of the unit above the surge figures (2153) is a well sorted sandy silt (Fig. 17) and its Inman (1952) parameters (Md_{Φ} = 5.95 and σ_{Φ} = 1.55) place it in the "fall" field of the Md_{Φ}/σ_{Φ} diagram (Walker 1971). Geochemistry of the middle (2153) and upper (2152) parts of the tuff unit indicates a rhyolitic magma (Tab. 1).

Tuffs of the Gombore II series

Several tuffs in secondary position, sands and silts rich in volcanics form the Gombore II succession. Well preserved tuff units occur at the bottom and the top of the sequence.

Tuff 9959/2151: This is present at the bottom of the channel of Gombore II above coarse alluvium with pumices and obsidian gravels and systematically below the archaeological layer. It shows vegetal

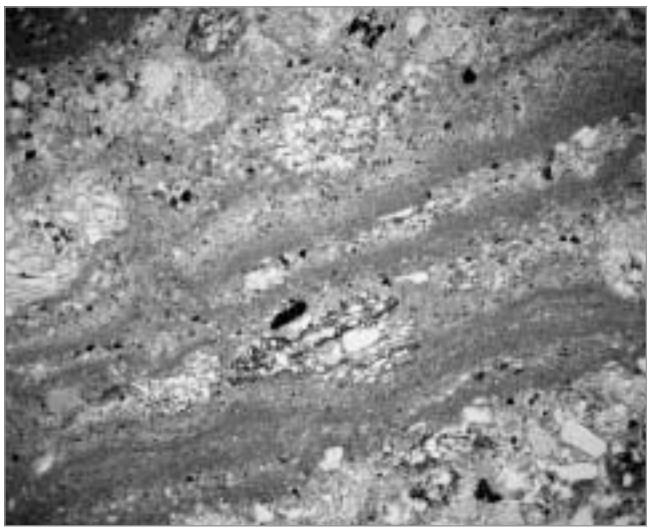

Fig. 25. Gombore II, tuff 2155/58 (sample 2158); microscopic view of layers rich in fibro-vacuolar pumices in natural light. *Cliché G. Kieffer*

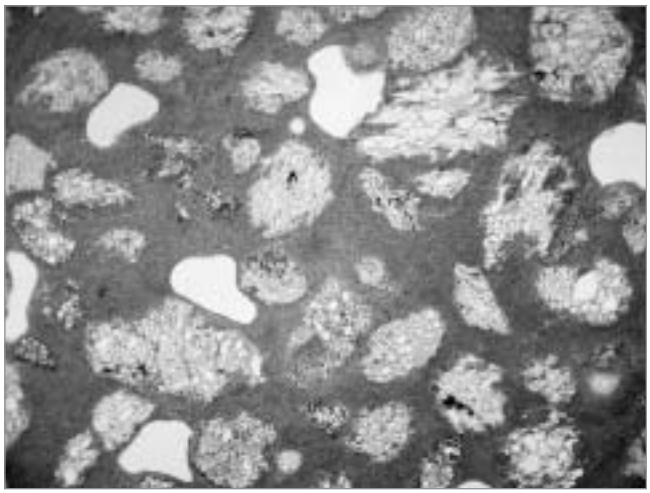

Fig. 26. Gombore II, tuff 2155/58 (sample 2158); microscopic view of vesiculated tuffs in natural light. *Cliché G. Kieffer*

Fig. 27. Garba IV, tuff 9911/15 ("Grazia Tuff"); thin white layer among the bottom alluvial sequence. *Cliché J.-P. Raynal*

imprints in some localities which indicate deposition in water. It is a well sorted silty sand (Fig. 24) and its Inman (1952) parameters (Md_Φ = 4.90/5.72 and σ_Φ = 1.83/1.65) place it in the "fall" field of the Md_Φ/σ_Φ diagram (Walker 1971). Its geochemistry indicates a dacitic magma (Tab. 1).

Tuff 9962: A tuffic unit with vegetal imprints is locally present above the archaeological layer. It is a well sorted sandy silt (Fig. 24) and its Inman (1952) parameters (Md_Φ = 2.60 and σ_Φ = 1.31) place it in the "fall" field of the Md_Φ/σ_Φ diagram (Walker 1971). Its geochemistry indicates a trachytic magma (Tab. 1). Even if there is no detailed description of the Gombore "tuff C" in literature, except for its controversial polarity (normal for Westphal 1979; reverse for Cressier 1980), tuff 9962 could be partly its equivalent.

A tuff unit caps the Gombore II series and overlies a complex of waterlaid cinereous tuff fossilizing an archaeological layer ("Butchery site"). This unit is probably the previously described "tuff D" of normal polarity (Chavaillon 1979c; Westpahl *et al.* 1979; Cressier 1980).

Tuff 9989/90: In thin section, we have a microconglomerate with beds either richer in feldspars and quartz or richer (even only made) in pumices. Pumices and pumice minerals are much bigger than mineral (fibrous and vacuolar) and more abundant. A lot of automorphe feldspars (alkaline and plagioclases). Very porous environment: a lot of voids and not jointed elements. Alteration deposits, mainly calcituous in coating between the minerals and pumice fragments. Not distant direct fall (pumices and minerals, quartz and feldspars). Its granulometry shows a bimodal composition of sands and silts (Fig. 24) and its Inman (1952) parameters (Md_Φ = 4.90 and σ_Φ = 3.27) place it at the limit of the "fall" field of the Md_Φ/σ_Φ diagram (Walker 1971). Its geochemistry indicates a dacitic magma (Tab. 1).

Tuff 2155/58: This is the same tuff unit as 9989/90 with peculiar aspects. In thin section, the obser-

ved sequence is stratified, very rich in fibro-vacuolar pumices (Fig. 25). But the whole is soaked in a very fine detritic matrix with however, a microconglomeratic bed. We note the presence of some mineral particles (from 1 to 2 mm). The very fine pelitic texture evokes that of dust deposits. Many vesicles are open within the fine matrix. We observe a variation in thickness and regularity in the identifiable beds. We have here surges deposits in the shape of vesiculated tuffs (Fig. 26). The granulometry shows a bimodal composition of silts and sands (Fig. 24) and its Inman (1952) parameters (Md_{Φ} = 6.20 and σ_{Φ} = 2.99) place it at the limit of the "fall" field of the Md_{Φ}/σ_{Φ} diagram (Walker 1971). Its geochemistry also indicates a dacitic magma too (Tab. 1).

Tuffs of the Garba series

Garba IV

From the bottom of the Garba IV section to the top of Garba gully, we have identified the following succession.

Tuff 9911/15: This tuff unit is located between archaeological layers Garba IV F and Garba IV D. It was previously identified as "Grazia tuff" and shows a clear reverse polarity (Cressier 1980). It is a 4 to 5 cm thick unit, light grey in color (5YR 7/1; Fig. 27). It is a well sorted sandy silt (Fig. 28) and its Inman (1952) parameters (Md_{Φ} = 5.00 and σ_{Φ} = 1.25) place it in the "fall" field of the Md_{Φ}/σ_{Φ} diagram (Walker 1971). In thin section (Fig. 29), it is a coarse microconglomerate of crystals in rather homometric sub-automorphic angular fragments (except for a few bigger elements), and especially alkaline feldspars. A few fragments of plagioclase, fibrous pumices and microlitic lavas and rare probable ferro-magnesium minerals (very weathered) are visible. The discontinuous and relatively

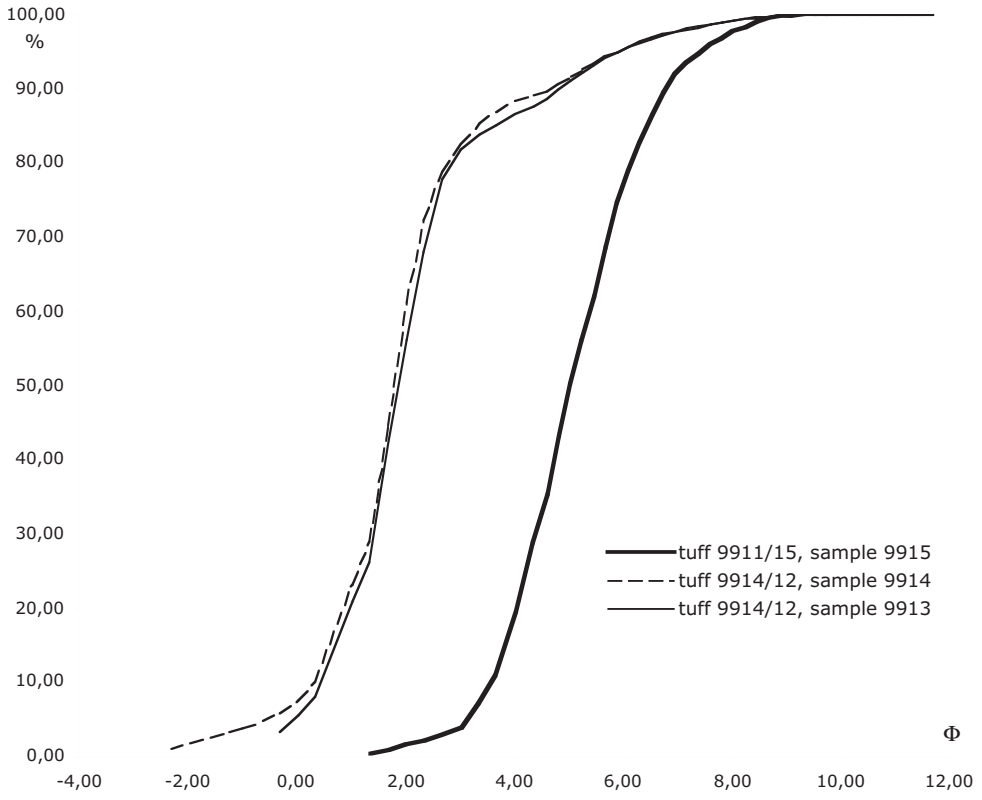

Fig. 28. Granulometry of Garba IV site tephras.

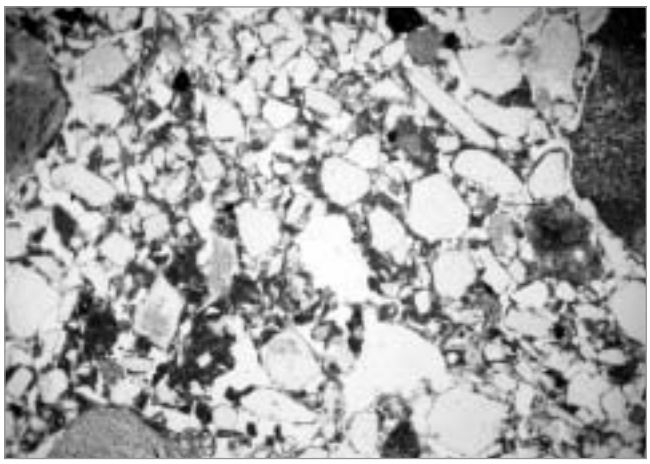

Fig. 29. Garba IV, tuff 9911/15 ("Grazia Tuff"; sample 9911); microscopic wiew in natural light. *Cliché G. Kieffer*

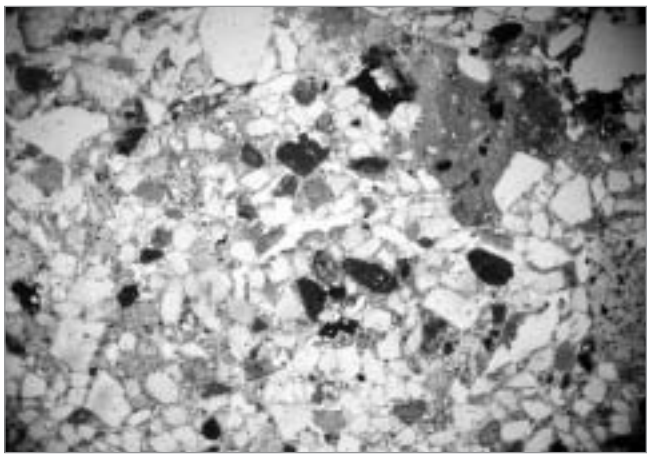

Fig. 30. Garba IV site, tuff 9914/12 (sample 9912); microscopic view in natural light. *Cliché G. Kieffer*

dense cement is probably calcitic in nature. Some voids and a considerable amount of alteration are present. These criteria indicate a distal fall of rhyolitic composition (Tab. 1). By its granulometry, geochemistry, microfacies and polarity, this tuff is *very similar* to tuff 9945/47 identified at the bottom of the Gombore I section (*see above*).

Tuff 9914/12: Thin layers (9914/13) interbedded and massively bedded (9912) are overlying Garba IV sands. Samples 9914 and 9913 are well sorted silty sands (Fig. 28) and their Inman (1952) parameters (Md_{Φ} = 1.80/1.86 and σ_{Φ} = 1.29/1.32) place them in the "fall" field of the Md_{Φ}/σ_{Φ} diagram (Walker 1971). In thin section (Fig. 30), the base of sample 9912 is micro-conglomeratic, mostly made of feldspathic elements in an abundant matrix (a sludge of heterometric minerals), with a few splinters of fibrous glass. General aspect is bedded with granulometry variations from one bed to another. The ratio of crystals to matrix varies. Some altered subautomorphic minerals are present, along with voids containing recrystallized minerals (zeolites?) but it is mainly calcite that has impregnated the block. We have here a more proximal fall, little reworked, perhaps co-ignimbritic (?). The upper

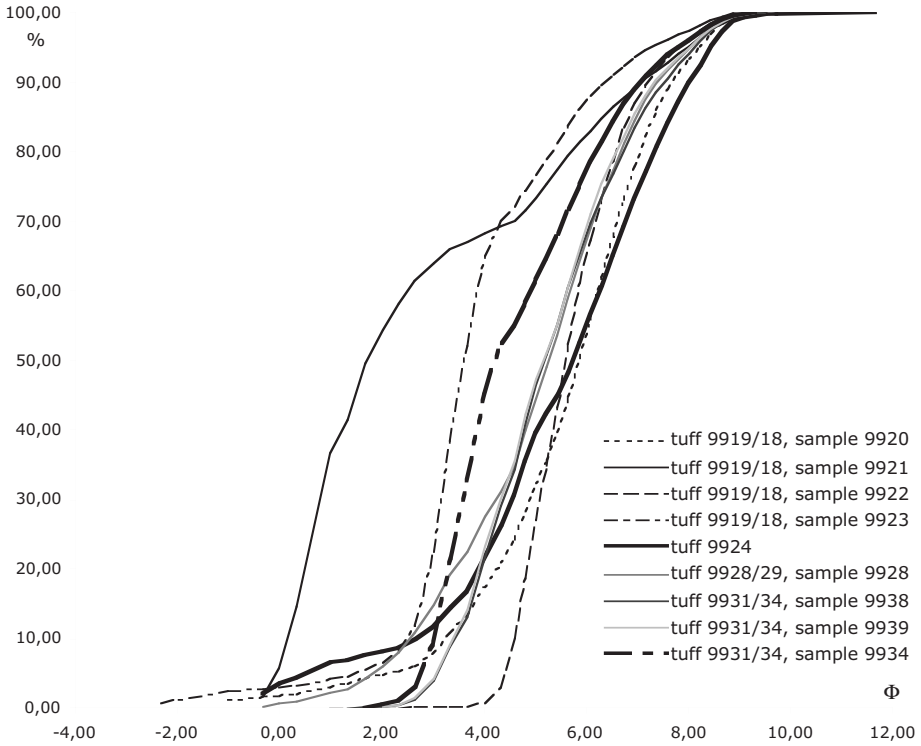

Fig. 31. Granulometry of Garba IV Gully tephras.

part comprises a more pelitic bed with a calcitic interstitial cement. From top to bottom: a microconglomerate without matrix (feldspathic minerals and quartz), a microconglomerate with matrix and a pelitic level at the base. This indicates direct falls. We have not performed chemical analysis on these tuff units that we supect to be reworked.

Tuff 9919/18: The bottom of this unit (sample 9920) is a well sorted sandy silt (Fig. 31) and its Inman (1952) parameters (Md_Φ = 5.85 and σ_Φ = 1.70) place it in the "fall" field of the Md_Φ/σ_Φ diagram (Walker 1971). In thin section, it is an essentially feldspathic microconglomerate, with more angular (broken) than automorphic elements. In the unit where the elements are bigger (and very altered) we note several fragments of highly altered lava of different types. The cement is calcitic. The whole is weathered and we note recrystallisation in the voids. We have here a direct or more or less reworked phreatomagmatic fall of rhyolitic composition (Tab. 1).

In thin section, the middle of the tuff is first an altered pelitic sequence with a vague stratification. Above is a thin micro-conglomerate with feldspathic angular elements (finer than those previously described) rather homometric in a fine matrix *pro parte* composed of fine glass splinters. It is a distal direct fall. This is confirmed by the granulometry of sample 9921: poorly sorted silty sand (Fig. 31) the Inman (1952) parameters (Md_Φ = 1.70 and σ_Φ = 2.91) of which place it in the "surge" field of the Md_Φ/σ_Φ diagram (Walker 1971). The upper part (Fig. 32) is an homometric micro-conglomerate with a matrix more or less rich in fine glass splinters according to beds. Elements are mainly feldspathic, angular, broken, and regularly distributed within the matrix. Alteration sometimes important with black and rust coloured products. We have here a distal direct fall. Granulometry confirms the differences observed between the beds. Sample 9922 is a very well sorted silt and sample 9923 is a well sorted silty sand (Fig. 31); their Inman (1952) parameters (Md_Φ = 5.60 and σ_Φ = 1.00 for 9922 and Md_Φ = 3.61 and σ_Φ = 1.44 for 9923 respectively) place them in the "fall" field of the Md_Φ/σ_Φ diagram (Walker 1971). Geochemistry varies

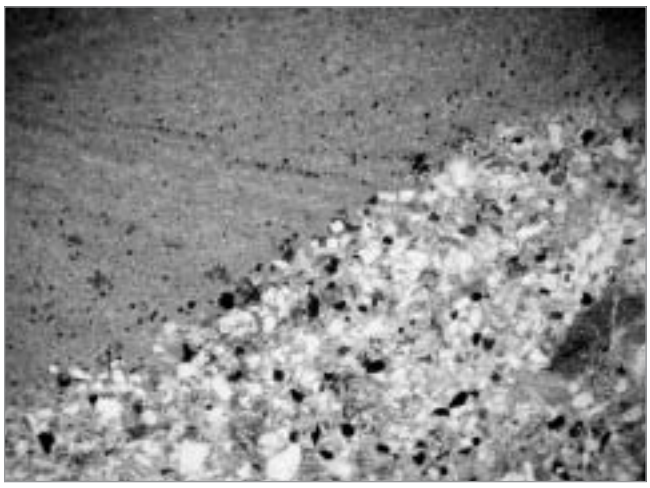

Fig. 32. Garba IV Gully, tuff 9919/18 top (sample 9918); microscopic view in natural light. *Cliché G. Kieffer*

Fig. 33. Garba IV Gully, fine deposit previously named "tuff A". *Cliché J.-P. Raynal*

Fig. 34. Garba IV Gully, tuff 9928/29, previously named "tuff B". *Cliché J.-P. Raynal*

Fig. 35. Garba IV Gully, tuff 9931/34, previously named "tuff C". *Cliché J.-P. Raynal*

from a rhyolitic (9922) to a dacitic (9923) composition (Tab. 1).

This tuff unit, previously described as "tuff A_0" is of reverse polarity (Cressier 1980) and is probably the "small tuff below tuff A" which has been dated by K/Ar on glass shards at 1.30 and 1.46 Ma (Schmitt *et al.* 1977).

Tuff 9924: This is a thin layer of well sorted sandy silts (Fig. 31) of dacitic composition (Tab. 1). Its Inman (1952) parameters (Md_Φ = 5.72 and σ_Φ = 2.00) place in the "fall" field of the Md_Φ/σ_Φ diagram (Walker 1971). As they contain abundant shells of lamellibranchia, this fall was trapped in water and slightly reworked.

Above tuff 9924 and up to tuff 9928, a two metres thick (at least) mass of reworked tephras more or less finely bedded, with concentrations of melanocratic minerals and clear vegetal bioturbations, has been previously named "tuff A" (Chavaillon 1979c; Fig. 33). Its polarity is reverse (Westphal *et al.* 1979; Cressier 1980) and K/Ar datings have been obtained on glass shards at 1.35 and 1.06 Ma (Schmitt *et al.* 1977). These ages can only be considered as a maximum age for the emplacement of the sediment. We do not understand why this particular layer has been chosen as a tuff-marker when others were much more distinctive and reliable. This certainly explains some of the difficulties encountered in establishing clear correlations between various sections.

Tuff 9928/29: This tuff unit is irregularly bedded, contains vegetal fragments and consists at its base (9928) of well sorted sandy silts (Fig. 31). Its Inman (1952) parameters (Md_Φ = 5.25 and σ_Φ = 1.90) place it in the "fall" field of the Md_Φ/σ_Φ diagram (Walker 1971). Towards the top (9929), silts are more sandy and poorly sorted (Fig. 31) and the Inman (1952) parameters (Md_Φ = 4.45 and σ_Φ = 2.52) place these in the "flow" field of the Md_Φ/σ_Φ diagram (Walker 1971). However, the hydromorphy and vertic aspect of this upper part of the unit throw some doubt on this interpretation which has to be confirmed by a further investigation of thin section (Fig. 34). This tuff unit 9928/29 appears to be what was previously named "tuff B" and presents a reverse polarity (Westphal *et al.* 1979; Cressier 1980).

Tuff 9931/34: A tuff unit approximatively one metre thick. It has been previously named "tuff C" and its polarity is reverse (Westphal *et al.* 1979; Cressier 1980). Several samples give a clear idea of the dynamic succession (Fig. 35).

Sample 9931: In thin section, the bottom part (sample 9931) is a microconglomerate with numerous feldspar crystals, subautomorphic for one part but largely broken (angular). Apparently no quartz present. Appreciable proportion of different types of microlitic lava in angular fragments. A few

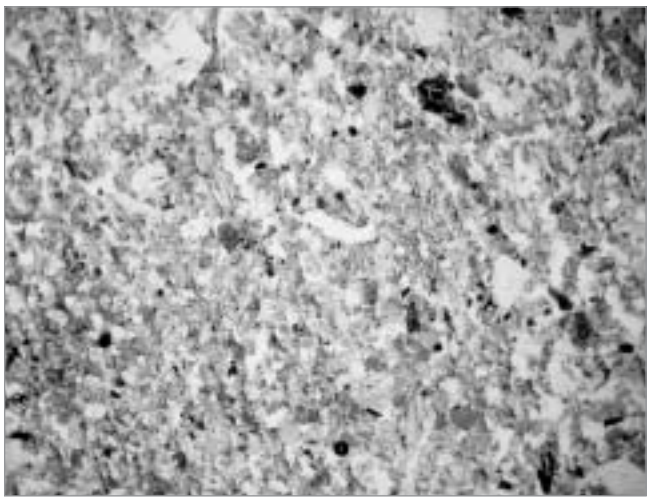

Fig. 36. Garba IV Gully, tuff 9931/34 (sample 9933).
Cliché G. Kieffer

pumices (vesicles). Many oxidised elements (opaque to rust coloured). Few ferromagnesians. A denticulate augite (weathered). No joined elements. Numerous intergranular voids. Biotite (?). This is a close phreomagmatic fallout (base).

Sample 9932: In thin section we see a mixture of heterometric elements in a very fine sludge. These are angular (broken) to automorphic (a few) but mostly subautomorphic elements. Quartz, alkaline feldspars and plagioclases present. Inclusions of microlitic lava. Pumices (bigger) fibrous to vacuolar. Local recrystallisation (in pumices or voids) zeolites? Oxidised elements (fragments of scoria?). Semi-distant fallout in phreomagmatic surge. At the top, we can see fine quartzo-feldsparic grains in a very fine sludge. A few light variations in the grains size. Continuation of the phreomagmatic fallout. This layer (sample 9938) is composed of well sorted sandy silts (Fig. 31) of rhyolitic composition (Tab. 1). Its Inman (1952) parameters (Md_Φ = 5.17 and σ_Φ = 1.61) place in the "fall" field of the Md_Φ/σ_Φ diagram (Walker 1971).

Sample 9933: In thin section, the base is microconglomeratic, with size variations of the elements according to beds, the elements being homometric in each bed, and this except for some rare elements a little bigger as some feldspaths and an old pumice (?) or an organism (?) very altered and recrystallized. Still vitreous fragments in the matrix of pelitic tendency, sludge aspect with all size but very small elements (Fig. 36). It is a distal direct fall, little reworked. Above, we can see a more or less pelitic sequence. Its lower part shows glass in its matrix as well as fine automorphe minerals (feldspath rods). It is the witness of a very distal direct fall.

Samples 9939 and 9934: The granulometric composition above (sample 9939) is still well sorted sandy silts (Fig. 31) which Inman (1952) parameters (Md_Φ = 5.17 and σ_Φ = 1.55) place in the "fall" field of the Md_Φ/σ_Φ diagram (Walker 1971). At the very top of this tuff unit, we observe a coarser laminae (sample 9934) with a bimodal mixture of silts and sands (Fig. 31) which Inman (1952) parameters (Md_Φ = 4.22 and σ_Φ = 1.65) still place it in the "fall" field of the Md_Φ/σ_Φ diagram (Walker 1971). One cannot exclude an hydraulic reworking of these upper beds.

Garba XII

At Garba XII, we have observed the following succession of tuff and tuff-like deposits, from the bottom to the top.

Tuff 9948/49: This unit which is more clearly bedded upwards and is composed of sandy silts, is less sandy at the top (Fig. 37) and Inman (1952) parameters (Md_Φ = 4.31/4.85 and σ_Φ = 1.05/1.31) place it in the "fall" field of the Md_Φ/σ_Φ diagram (Walker 1971). This unit is of dacitic to rhyolitic composition (Tab. 1). It has been previously named "tuff A" and has a reverse polarity (Chavaillon 1979c; Westphal *et al.* 1979; Cressier 1980).

Tuff 9941/42: At the base of this unit, we first observe in thin section a microconglomerate with potassic feldspar, rare plagioclases, debris of various microlitic lavas. A porous unit. Dispersed elements.

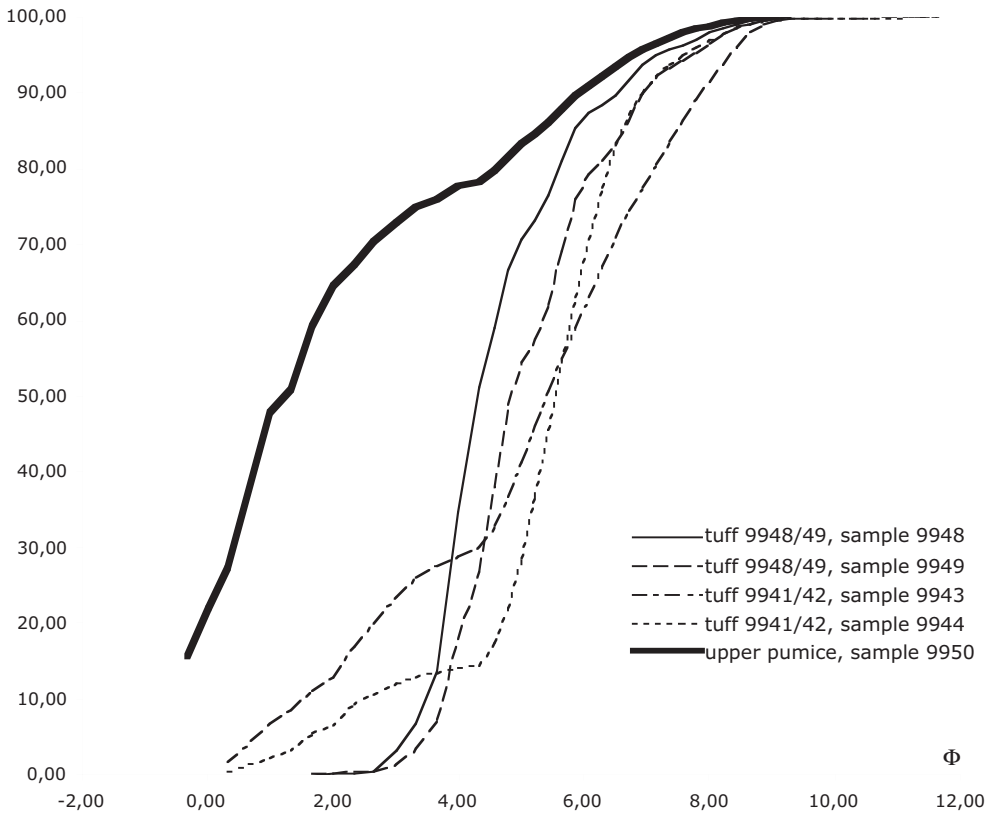

Fig. 37. Granulometry of Garba XII tephras.

Important rust coloured alteration. This is a phreatomagmatic semi-distal fall of andesitic composition (sample 9943; Tab. 1), bimodal mixture of sands and silts poorly sorted (Fig. 37) and Inman (1952) parameters (Md_{Φ} = 5.40 and σ_{Φ} = 2.55) place it in the "fall" field of the Md_{Φ}/σ_{Φ} diagram (Walker 1971).

Above, we first observe in thin section a sludge with a very fine matrix (pelitic). Very small broken elements (quartz and/or feldspars). A few rare large fibrous pumices. Then we observe a stratified pelitic sequence. Minute quartz or feldspar grains. A much larger fibrous pumice followed by two small beds with much bigger vacuolar or fibrous pumices (millimetric) (beds thickness <0.5 cm). This is followed by a more than 1 cm thick bed where pumices are embedded in the pelitic mass. The top is still pelitic. This indicates a very fine alluviation. This deposition of mud in very calm conditions occurred during a rather distant eruptive context (pumices production during the sedimentation). We have a well sorted bimodal mixture of sands and mainly silts (sample 9944; Fig. 37) whose Inman (1952) parameters (Md_{Φ} = 5.55 and σ_{Φ} = 1.06) still place it in the "fall" field of the Md_{Φ}/σ_{Φ} diagram (Walker 1971). The composition is dacitic (Tab. 1), very rich in Ba as in the bottom part of the tuff unit.

At the top, we see in thin section a very fine pelitic unit with vacuolar pumices scattered in the mass or in older beds deformed by moves posterior to their deposition. Pseudo load-casts against the pumices. Pelitic unit perhaps remobilized in a muddy movement after its primary deposit.

This tuff unit has been previously named "tuff B" and has a reverse polarity (Chavaillon 1979c; Westphal *et al.* 1979; Cressier 1980).

Tuff 9950: This unit is a pumice fall which caps the section at Garba XII. Further investigations are necessary to precise its relationships with other pumice falls observed in similar topographic and stratigraphic position for example Gombore II "Butchery site", Tuka, Kella or Simbiro.

The non-welded ignimbrite

Fig. 38. Degassing pipes in non-welded ignimbrite at Melka Garba. *Cliché G. Kieffer*

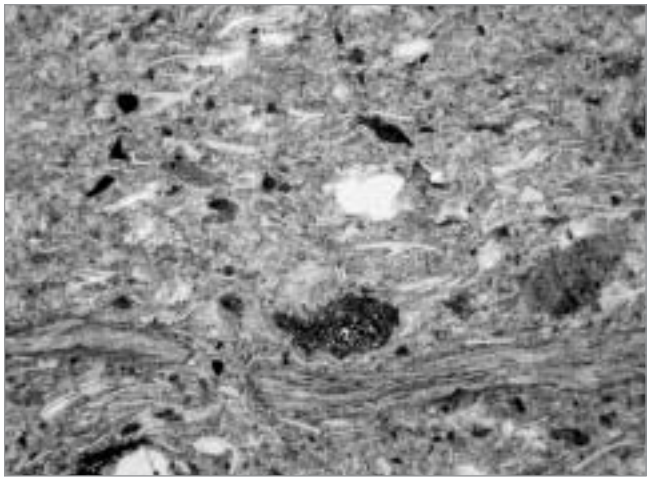

Fig. 39. Tinishu-Kersa, non-welded ignimbrite (sample 9933); microscopic view in natural light. *Cliché G. Kieffer*

The next volcanic episode of regional importance is that of the non-welded ignimbrite, previously described as ignimbritic tuffs (Taieb 1974), which seems to have occupied quite differentiated topography, at least against the welded ignimbrite, with a well-settled drainage pattern, as witness the Kella, Melka Garba and Tinishu-Kersa outcrops. Without doubt several phases, with presently unknown origins, are responsible for the setting of the characteristic facies with ground surge and degassing pipes (Fig. 38), and a thickness averaging from three to five metres. It seems possible that a recent phase, perhaps the last of notable importance, could be at the origin of the large sheet of non-welded ignimbrite, which is present at Melka Garba, on the right bank of the Awash, and is found again more widely spread downstream on the left bank. Several localities have been studied from a microfaciological point of view:

Tinishu-Kersa (sample 9902): Vitroclastic structure, felt like glass splinters (at least 80% of the rock), little fluidal structure at the thin section scale. A few fibrous pumices generally elongated, a few rarer vesicular pumices, wrapped in the felt of splinters, rare crystals of alkaline feldspath and a few flakes. Perhaps a zircon (?). Alteration with rust to black products. Bubbles or voids more or less filled with zeolites (?). This formation is mineralogically different from the underlying welded ignimbrite (9901) because of the rarity of feldspars.

Tinishu-Kersa (sample 9903): Many similarities with sample 9902. Glass splinters often cuneiform. Aspect a little more fluidal. Rare alkaline feldspaths. A lot of alteration and recrystallisations (Fig. 39).

Melka Garba (sample 9908): Finely vitroclastic structure with fragments of fibrous or vesicular pumices, the latter more numerous and a little bigger. Structure almost not fluidal apart from the moulding of the biggest pumiceous elements. Fine devitrification, very little feldspath crystals in small flakes. Similar alteration, a few recrystallisations (zeolites, calcite?).

Pumices from this ignimbrite sampled at Melka Garba have a chemical composition which refers to a rhyolitic magma (sample 9910 in Tab. 1), as noted previously (samples 236 from Kella 1 and 142 from Tuka in Tab. 1 after Taieb 1974). A K/Ar age of 0.72 Ma "which should be interpreted cautiously given the young age of the sample and the lack of a repeat anlysis" was obtained on this unit of reverse polarity (sample ET-75-5, Schmitt *et al.* 1977). The reverse polarity of this unit (also described as "tuff B" in different papers) has been confirmed by a detailed analysis of several samples taken at Kella, Karre and

Melka Garba (Cressier 1980). Thus this unit belongs clearly to the Matuyama Polarity Zone with a minimum age of 0.78 Ma.

The setting of this ignimbrite could have been accompanied by explosive events and the development of surges, responsible for a series of tuff levels present in capping position in the sections of Gombore I and Garba IV and seem to have fit, as the concerned ignimbrite, the topography close to the present one (*see supra*). Based upon macro and micro-facies and on preliminary geochemistry analysis, the correlation with so-called "tuff B" of Gombore I and "tuff C" of Garba IV, both of reverse polarity, is quite reasonable.

Apart from the subsident zones, this episode is responsible for the general topographic regularisation of the basin, as it can be observed nowadays out of the Melka Kunture area. It is after the placement of the non-welded ignimbrites that the main fault reactivation takes place, it is quick and with an important displacement. The recent and present erosion has cleared the main fault plane in several points. The visible rocks on the default plane were fossilised on the top and are not visible even in the erosive incisions of the collapsed compartment, giving witness to the vigour of the reactivation.

Conclusions

As for Pompei, Herculanum and a few other archaeological areas, the volcanism fossilised and conserved the Melka Kunture prehistoric sites. The depression, created upstream of the Awash village sill and maintained by the tectonic reactivation of the fault system that constitutes the south-south-east border, provided a choice receptacle for the volcanic materials.

Except for the products of the initial autochthonous manifestations, the latters came from volcanoes distant by several kilometres and up to several tens of kilometres. The volcanoes were mostly explosive, as indicated by the differentiated nature of the magmas. In multiple phases of activity, since 4 or 5 million years ago, they have mainly emitted pyroclastites. A good quantity arrived directly on the sites, particularly the various welded or non-welded ignimbrites but also numerous aerial ashy and pumiceous fallouts, from repeated phreato-magmatic blows, whose destructive strength is well known. The periods of human occupation, less than 2 Ma old, are posterior to the large eruptions that produced the wide sheets of welded ignimbrites. Such occupations were however disturbed by the very violent eruptions that have on several occasions, completely erased any evidence of the existence of hominids along the Awash River, particularly those of non-welded ignimbrites. The several tuff layers identified in the Gombore-Garba series support the simple model previously established. Moreover, correlations between localities are difficult to establish due to lateral variations in facies and geochemistry of tephras. A preliminary synthesis is proposed (Tab. 2).

The Awash River and its tributaries, that allowed the occupation by prehistoric populations, have existed since at least 4 to 5 Ma. It regularly re-established its course after each important volcanic manifestation and established a new basal level. The water flows of this river and its tributaries provided the mechanism that drove the sedimentation of reworked volcanic materials and fossilised and conserved the archaeological sites.

This sedimentation was a consequence of the border faults reactivation that provoked on several occasions the subsidence of the basin upstream of the Awash sill. This process was assisted by the arrival of volcanic material during eruptions that considerably augmented the river's load. The erosion resumed its digging following each filling. However, this cycle was largely controlled by the level of the Awash sill, at the exit of the basin which may have remained high for a long period of time, limiting the possibility of local erosion. Its position upstream of the river gorges made it remote from the regressive erosion proceeding upstream from these gorges untill recently.

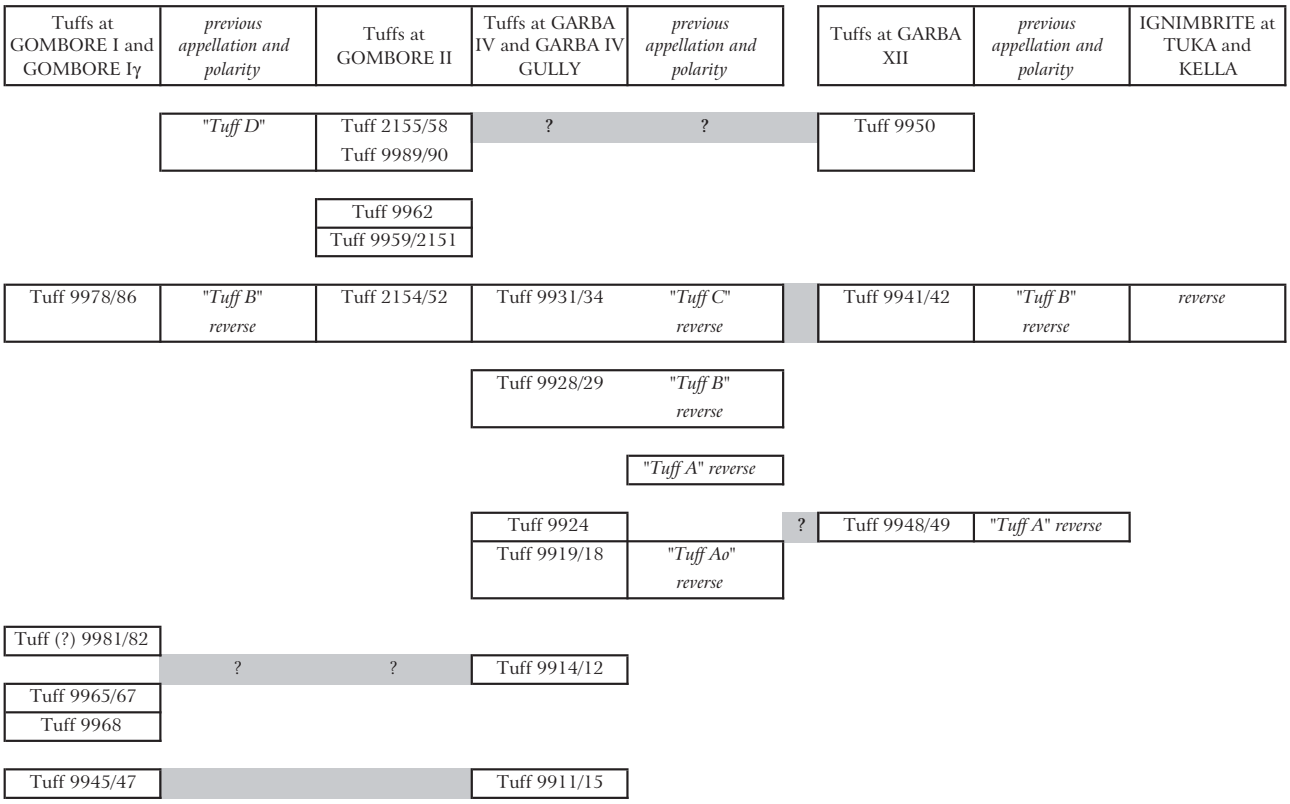

Tab. 2. The tuffs sucessions at Gombore and Garba. A preliminary attempt of correlations.

Acknowledgements

Financial support for field work and laboratory analyses was provided by CNRS (GDR *Hommes et volcans avant l'histoire*), Région Aquitaine and Région Auvergne for project *Espaces volcaniques préhistoriques* and Italian Archaeological Mission at Melka Kunture. We are grateful to Marianne Hirbec-Raynal for the English translation and to Peter Bindon for its revision. We thank Geneviève Papy who performed the granulometric analysis of tephras, Mosshine El Graoui who prepared most of the thin sections, Bernard Martin for his last minute help and Jacques Morel at S.A.R.M. in Nancy who performed the geochemical analysis of tephras.